Available online at www.sciencedirect.com
ScienceDirect
Gene 398 (2007) 177–182
GENE
www.elsevier.com/locate/gene

The molecular heterogeneity of hemocyanin: Structural and functional properties of the 4×6-meric protein of *Upogebia pusilla* (Crustacea)

M. Paoli [a], F. Giomi [a], N. Hellmann [b], E. Jaenicke [b], H. Decker [b], P. Di Muro [a], M. Beltramini [a,*]

[a] *Department of Biology, University of Padova, Padova, Italy*
[b] *Institute of Molecular Biophysics, University of Mainz, Mainz, Germany*

Received 11 December 2006; received in revised form 8 February 2007; accepted 14 February 2007
Available online 25 April 2007

Abstract

The structural properties of the hemocyanin isolated from the Mediterranean mud shrimp, *Upogebia pusilla* (Decapoda: Thalassinidea), were investigated. Our intent was to make use of the *U. pusilla* case to perform a structural comparison between crustacean and chelicerate 4×6-meric hemocyanins. The thalassinidean hemocyanin appears similar in size but different in structural organization compared to the chelicerate 4×6-mer. Ultracentrifuge analyses on the purified protein revealed a sedimentation coefficient of 39S, typical of 4×6 hemocyanins. Electron micrographs are in agreement with a model in which four 2×6-meric building blocks are arranged in a tetrahedron-like quaternary structure and not in the quasi-square-planar orientation characteristic of the chelicerate protein. Size-exclusion chromatography-fast protein chromatography analysis showed elevated instability of the protein in absence of divalent ions or at pH values higher than 8.0. This analysis also shows that the dissociation of the *U. pusilla* 4×6-meric hemocyanin into hexamers occurs without any intermediate 2×6-meric state, in contrast with the dissociation profile of the chelicerate protein exhibiting several dissociation intermediates. The oxygen-binding properties of *U. pusilla* hemocyanin were studied to disclose possible effects by the typical allosteric effectors that modulate the functional properties of crustacean hemocyanin. A marked Bohr and lactate effect, but no significant influence of urate, on the oxygen affinity of *U. pusilla* hemocyanin were found.

Keywords: Hemocyanin; Quaternary structure; Dissociation; Oxygen binding; Catalytic properties

1. Introduction

Hemocyanins (Hcs) are giant oligomeric oxygen carriers present in the hemolymph of arthropods and molluscs. In arthropods, polypeptide chains with M_R of about 75 kDa, each containing one dinuclear copper oxygen-binding site, represent the functional and structural subunits. Arthropod Hcs, however, are generally found as oligomers where 6 subunits aggregate to form in general hetero2×6-meric complexes. More hexamers may eventually be combined into 2×6, 4×6, 6×6 or 8×6 oligohexamers. The particular aggregation form, in which the oxygen carrier is found, is highly species dependent, and more than one form may coexist in the same species (Markl and Decker, 1992). Significant differences in primary structures exist within the different subunits building the heterohexamers found in one species as well as within the Hcs subunits of different species. Within Crustacea, 2×6 and hexameric (1×6) Hcs are generally found: notably the former is the characteristic aggregation form of portunid crabs, the latter of caridean, peneid, pagurid and palinuran decapod species (Markl, 1986).

In the context of Crustacea, the thalassinidean shrimps represent a unique case since they carry a 4×6-meric Hc. Comparative studies on the association state of these Hcs revealed a main component with 39S sedimentation coefficient, which corresponds to the 4×6-mer of chelicerates (Roxby et al., 1974; Miller and van Holde, 1974; Miller et al., 1977; Ellerton et al., 1983; Miller and van Holde, 1982; Taylor et al., 2000). In addition, a minor pool of Hc in the 1×6-meric form (17S) was described. A 2×6-meric intermediate form (25S) was found notably for members of the family of Upogebiidae, *U. pugettensis* (Miller et al., 1977) and *U. deltaura* (Taylor et al., 2000).

Abbreviations: EDTA, ethylene diamine tetra-acetic acid; EM, electron microscopy; FPLC, fast protein liquid chromatography; Hc, hemocyanin; SEC, size-exclusion chromatography; TEM, transmission electron microscopy.

* Corresponding author. Department of Biology, University of Padova, Viale G. Colombo 3, I-35131 Padova, Italy. Tel.: +49 827 6337; fax: +49 827 6300.
E-mail address: mariano.beltramini@unipd.it (M. Beltramini).

0378-1119/$ - see front matter © 2007 Elsevier B.V. All rights reserved.
doi:10.1016/j.gene.2007.02.035

The 4×6-meric Hcs are present also in chelicerates. The physico-chemical properties of the protein isolated from the tarantula *Eurypelma californicum*, have been thoroughly investigated. While the native protein is characterized by a sedimentation coefficient of 37S, several oligomers can be singled out in dissociation experiments (Markl et al., 1982; Savel-Neimann et al., 1988; Voit et al., 2000).

Two models are known for the ikosatetrameric Hc: the first one refers to chelicerate 4×6-mers, fully described for the scorpion *Androctonus australis* (Lamy et al., 1981) and the tarantula *E. californicum* (Erker et al., 2006; Voit et al., 2000); the second model has been proposed to describe the thalassinidean shrimps Hc, notably in *Callianassa californiensis* (Cavellec et al., 1990). It was shown by multivariate statistical analysis applied to computer aligned electron microscopic images that the 4×6 Hcs of *A. australis* and *E. californicum* are very similar (Bijholt et al., 1982) and fit the model earlier derived for the 4×6 half molecules of *Limulus polyphemus.* Such 4×6-mers are quasi-square-planar and comprise two 2×6-meric halves in an antiparallel arrangement that come in contact edge-to-edge, leaving a "deep cleft" between them (Martin et al., 2007). No high-resolution structure is available for the crustacean 4×6-mer but electron microscopy (EM) analysis revealed a completely different quaternary structure. EM analysis displayed a characteristic triangular shape and a three-dimensional model was constructed to combine a 4×6 aggregation state with the triangular profiles observed in the electron micrographs. The model consists of four 1×6-meric building units associated in a tetrahedron-like structure (Cavellec et al., 1990). Thus, while both in thalassinidean shrimps and chelicerates 4×6-meric Hcs exist, their quaternary structures seem to be very different.

The oxygen-binding properties of Hcs, that define their physiological role as oxygen carriers, are modulated by protons and organic ions such as lactate and urate. The effects of pH and organic ions were intensively studied on crustacean and chelicerate Hcs and different responses in the two *phyla* were described. Protons affect the oxygen-binding properties of both crustacean and chelicerate Hcs. In contrast, lactate and urate exert their effect on crustacean Hcs but not on chelicerate proteins. Within Crustacea, however, not all species exhibit this effect: in particular, no lactate effect was reported for thalassinid shrimps *Colocaris macandreae* (Taylor et al., 2000) and *Neotrypaea* (*Callianassa*) *californiensis* (Mangum, 1983).

Our focus in this work was the structural characterization of the Hc isolated from the thalassinid shrimp *Upogebia pusilla* in order to generalise the model of a thalassinid-specific hexamers arrangement, the association–dissociation behaviour and the oxygen-binding properties of this 4×6-meric Hc in comparison to the 24-mers found in chelicerates. Furthermore, we have investigated the oxygen-binding properties of *U. pusilla* Hc, with the aim to add further information on the lactate and urate effect on thalassinid shrimps Hcs.

2. Materials and methods

Living specimens of *U. pusilla* were purchased from local fishermen at Porto Levante on the Adriatic Sea in the proximity of the delta of the river Po. The hemolymph was collected by means of a needle inserted into the pericardium of living animals. The hemolymph, sampled from N=250/300 individuals, was stored at 0 °C after addition of protease inhibiting cocktail (Sigma-Aldrich Art. P2714). The samples were successively dialyzed against stabilization buffer (Tris 100 mM, $CaCl_2$ 20 mM, pH 7.6) and subsequently centrifuged at 45,000 *g* for 25 min (Beckman J2-21) for the removal of cells and other suspended material. The Hc was finally isolated by sedimentation at 296,000 *g* for 5 h in a Beckman ultracentrifuge XL-70. After purification, the pellet was resuspended in the same buffer and stored at −20 °C in the presence of 20% (w/v) sucrose. Before use, Hc was further purified by size-exclusion chromatography (SEC) carried out with a Sephacryl S-300 XK 26/60 column (Pharmacia). Elution was performed at low pressure and regulated by a BIORAD BioLogic DuoFlow FPLC device with stabilization buffer at 1.3 mL/min. Before chromatography, the protein was dialyzed against stabilization buffer. Fractions exhibiting an absorbance ratio A_{338}/A_{280}=0.21–0.25 were pooled and used for further analysis.

Both the Bradford and the Lowry assays were employed to determine the extinction coefficient of *U. pusilla* Hc. Two different Hcs standards were used to calibrate the colorimetric assay: *E. californicum* Hc, which has about the same size of *U. pusilla* Hc but belongs to the group of chelicerates; and *Carcinus aestuarii* Hc, a 2×6-mer but phylogenetically more closely related to the studied Hc. The concentrations of standard Hcs in the samples used to calibrate the assays were determined using the coefficients: 1.10 mL mg^{-1} cm^{-1} for *E. californicum* Hc (Loewe, 1978) and 1.24 mL mg^{-1} cm^{-1} (Dainese et al., 1998) for *C. aestuarii* Hc. The Bradford and the Lowry assays were used to determine the concentration of *U. pusilla* Hc solutions used to record the absorption spectrum. By this approach it was possible to calculate an extinction coefficient at 278 nm of 1.11±0.05 mL mg^{-1} cm^{-1} for *U. pusilla* Hc.

Aggregation state was determined by comparing *U. pusilla* Hc SEC-FPLC elution profile with the elution profiles of *Palinurus elephas* 1×6 Hc, *Astacus leptodactylus* 2×6 Hc and *E. californicum* 4×6 Hc. Chromatography was performed in the buffer above described with a Sephacryl S-300 XK 26/60 column (Pharmacia). Dissociation experiments were carried out with the column as above using 50 mM Tris/HCl buffer at various pH values and in the presence of 10 mM EDTA. Ion exchange chromatography was performed on a Resource Q column equilibrated with 50 mM Tris/HCl, 10 mM EDTA pH 9.2.

The aggregation state was also determined by sedimentation velocity analysis performed with a Beckmann XL-I analytical ultracentrifuge. For each analysis, 400 μL of 0.7 mg/mL purified sample were employed. The experiments were carried out at 25,000 rpm (rotor Beckman type 60 TI) for 100 min and 50 measurements (at 2 min intervals each) were performed at wavelengths of 278 (and 338 nm). The data were processed with the freeware UltraScan II v.7.2 (Borries Demeler and University of Texas System). The sedimentation constants given correspond to the values extrapolated for 20 °C and water ($S_{20°,w}$).

Transmission electron microscopy (TEM) analysis was carried out on a Hitachi H600 electron microscope. Diluted aliquots of Hc

preparations were absorbed onto glow-discharged carbon-coated butwar films on 400-mesh copper grids. The grids were negatively stained with 1% uranyl acetate and observed at ×40,000.

Oxygen-binding curves were recorded using the fluorimetric polarographic method (Loewe, 1978). In this method, the sample, initially completely oxygenated, is slowly fully deoxygenated by a stream of water-saturated nitrogen flow, while oxygen partial pressure is measured with an oxygen microelectrode (Microelectrodes Inc, NH, USA). Simultaneously, a photoamplifier records the fluorescence variation of the sample due to the relative variation of oxygenated Hc. All measurements were performed at 20 °C on 850 µL samples of 0.20–0.25 mg/mL Hc in buffer. Before and after every oxygen-binding curve, an emission spectrum of the sample, excited at 278 nm, was recorded in the range from 290 to 400 nm to check for the integrity of Hc: the protein excited at 278 nm shows an emission peak at about 330 nm.

3. Results and discussion

3.1. Quaternary structure and stability

U. pusilla Hc elutes in size-exclusion chromatography (SEC), in buffer at pH 7.6, 4 °C and containing Ca^{2+} ions, as a single peak, as shown in Fig. 1 where the chromatographic pattern of the investigated protein is reported together with the profiles obtained with other arthropod Hcs. By reference to such standard proteins of known quaternary structure (4×6-meric Hc from *E. californicum*; 2×6-meric Hc from *A. leptodactylus*, 1×6-meric Hc from *Panulirus elephas*) a 4×6-meric aggregation state can be inferred.

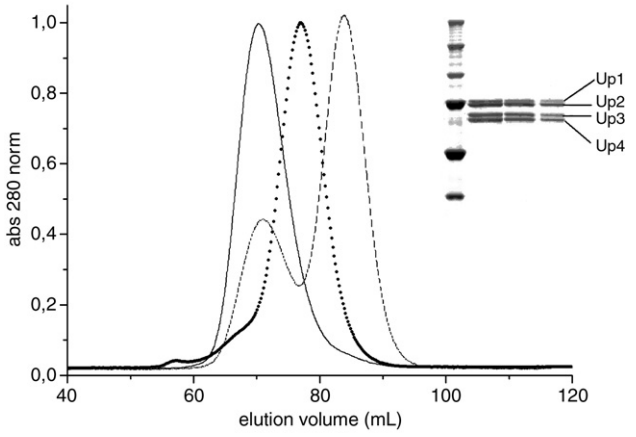

Fig. 1. Structural characterization of *Upogebia pusilla* hemocyanin. A: SEC-FPLC elution profiles in Sephacryl S-300 XK 16/60 column of the *U. pusilla* hemocyanin (solid line), the 2×6-meric hemocyanin of *Astacus leptodactylus* (dotted line), and a mixture of the 1×6-meric hemocyanin of *Palinurus elephas* and of the 4×6-meric Hc of *E. californicum* (dashed line). Elution buffer: 100 mM Tris, 20 mM $CaCl_2$, pH 7.6. The various chromatographic profiles were obtained in separate runs, performed under the same conditions (for details see Materials and methods) and were normalized to the same maximum absorbance at 280 nm. Inset: SDS-PAGE of unfractionated *U. pusilla* hemocyanin, markers from top to bottom: 250, 150, 100, 75, 50, 37 kDa (Bio-Rad Precision Plus Protein Standard). The protein applied to the three Hc lanes is (from left to right) 7.3 µg, 5.5 µg and 3.7 µg, respectively.

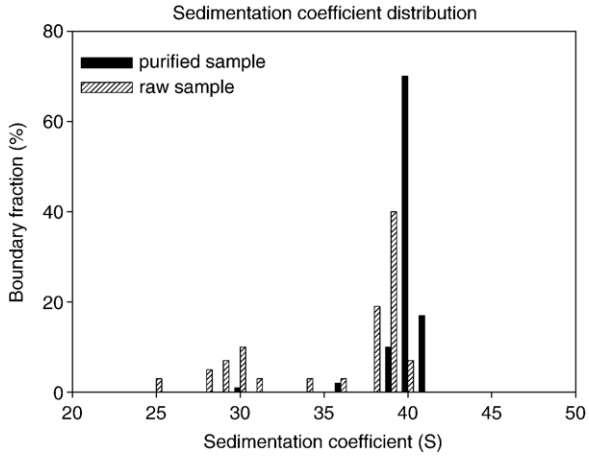

Fig. 2. Histogram of the values of sedimentation coefficient found for *Upogebia pusilla* hemocyanin purified. The data were acquired either on the whole hemocyanin preparation (shaded bars) or on the hemocyanin purified throughout SEC-FPLC and isolated from the centre of the chromatographic elution peak (black bars). These latter data are in complete agreement with the sedimentation coefficient values obtained for the samples taken from right and left shoulders of the elution peak (data not shown). Buffer: Tris 50 mM, $CaCl_2$ 20 mM, pH 7.6.

Ultracentrifugation analysis of unfractionated Hc preparation (Fig. 2) shows two components: a main component with a sedimentation coefficient of 39S is found together with a minor component of 29S. The value of the former is compatible with a 4×6-meric aggregation state and it is found also in the case of the chelicerate Hc (*E. californicum,* Markl et al., 1976) and of the Hc from other thalassinidean shrimps (Arisaka and van Holde, 1979; Taylor et al., 2000). The sedimentation coefficient of the minor component suggests an aggregation state intermediate between the 4×6-meric and the 2×6-meric and it has been found *in vitro* also in the case of *E. californicum* Hc. Here, the 19-mer is an artifact not occurring in nature. It consists of three intact hexamers, while the fourth hexamer lost up to five subunits by dissociation (Savel-Niemann et al., 1988). It contributes to the chromatographic pattern of the *U. pusilla* whole Hc in broadening the main 4×6-meric Hc peak. It does not represent a species in equilibrium with the 4×6-meric Hc since the sedimentation coefficient determination of the Hc previously purified by SEC-HPLC shows only the 39S material (Fig. 2). The 29S-material was not further investigated due to its low concentration with respect to the main 4×6-meric form.

The 39S component of the hemolymph from *U. pusilla* Hc was further investigated in order to obtain details on the arrangement of the building blocks within the quaternary structure. To this aim, transmission electron microscopy (TEM) was used. A typical field obtained by negative staining TEM analysis is reported in Fig. 3 together with a gallery of higher magnifications of selected images. From left to right, the first inset shows a simple globular shaped object of about 10 nm across, which represents the 1×6 form of the Hc. The second inset reports the image of a dimeric profile with twice the size of the previously described hexamers. The last three insets refer to the most common aggregation form of *U. pusilla* Hc found in the TEM field, namely the 4×6-mer. This aggregation state accounts for about 80% of total hexamers present in the protein

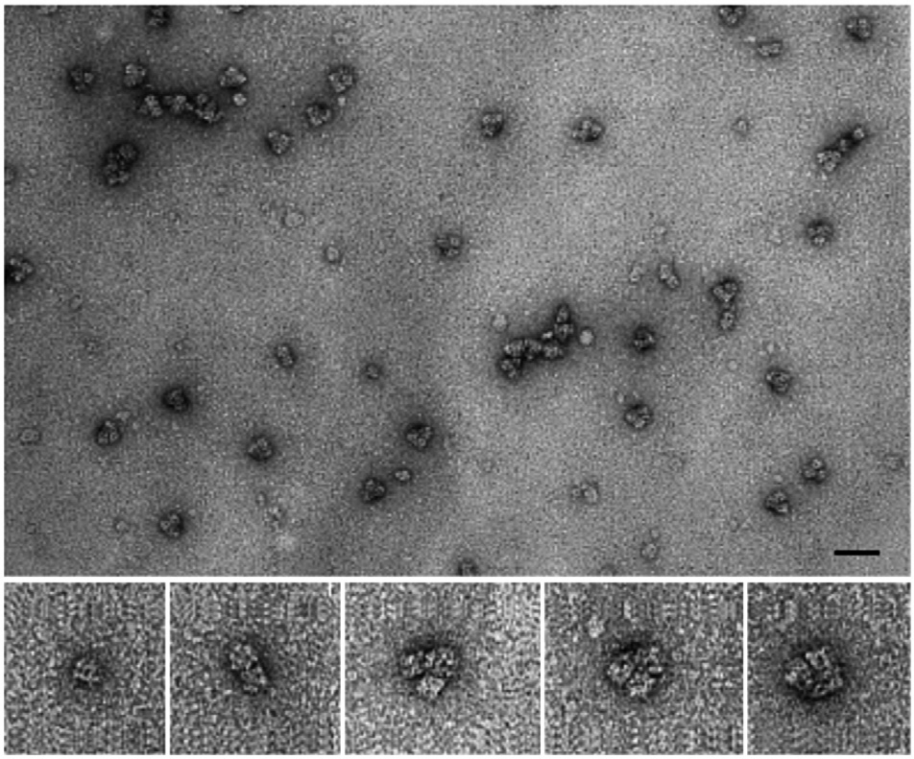

Fig. 3. Electron micrographic field of *Upogebia pusilla* hemocyanin stained with 1% uranyl acetate and observed at a magnification of 40,000. The scale is 50 nm. The five insets show higher magnifications (250%) of different aggregation forms; from left to right: 1×6-meric (first inset), 2×6-meric (second inset); the insets 3–5 represent different orientations of the 4×6-meric Hc.

pool, while 10% forms 2×6-mers and 10% is found as 1×6-mer. The shape, different from the quasi-square-planar one found for chelicerate 4×6 Hc, is fully compatible with the top view of a quaternary structure where each 2×6-meric building block is arranged as to form a tetrahedron, in agreement with the model proposed for the other thalassinidean shrimp *C. californiensis* (Cavellec et al., 1990). The presence of hexamers and 2×6-mers in the same fields together with the 4×6-meric whole molecules may be due to dissociation effects of Hc induced by the uranyl acetate staining used for the electron microscopy. In agreement, TEM fields recorded in the presence of 20 mM Ca^{2+} reveal almost only Hc in its 4×6-meric native state (data not shown), underlining both the stabilization effect of calcium and the instability of the Hc quaternary structure.

In this frame, the issue of the stability of the oligomers was also addressed by means of SEC-FPLC experiments carried out under dissociating conditions. The elution profiles of Hc reported in Fig. 4A reveal that the 4×6 Hc peak is lost upon removal of calcium at pH 7.6 and the protein dissociates to hexamers. The same effect is observed in the presence of 20 mM $CaCl_2$ but increasing the pH to 8.0 (data not shown). These results show that the aggregation state of *U. pusilla* 4×6-meric Hc is governed by both pH and Ca^{2+}, in agreement with previous work on *C. californiensis* Hc (Miller and van Holde, 1974). Under our experimental conditions, the hexamers represent the first dissociation products of 4×6-mers and point to a dissociation pattern different from that of the 4×6-meric Hc of chelicerates. In the case of *E. californicum*, the two heterodimers consisting of subunits b and c build a ring connecting the four hexamers: dissociation products such as 19-mers, 14-mer and 7-mers and no multiples of hexamers can be isolated as distinct species along the dissociation pathway of the whole Hc (Markl et al., 1981; Savel-Niemann et al., 1988). Thus, *U. pusilla* Hc can be defined as a tetramer of 1×6-meric building blocks, in contrast to the 4×6-meric Hc of Chelicerates where strong interactions exist between hexamers to build up the 2×6-meric half molecules. In the case of tarantula, scorpion and horseshoe crab Hcs the quaternary organization depends on a precise topology of the distribution of the various subunits within the oligomer (Lamy et al., 1981; Markl et al., 1981; Markl and Decker, 1992; Voit et al., 2000; Martin et al., 2007). In particular, linker subunits are responsible for the aggregation of the two 2×6-mers and for the highly hierarchical order of interactions (Voit et al., 2000). No equivalent information is available in the case of thalassinidean shrimps yet. In this frame, the elucidation of the sequence of each polypeptide chain of monomers is under way. Previous studies on thalassinid shrimps Hc demonstrated the presence of 2×6-meric Hc in some upogebid species (*Upogebia pugettensis* and *Upogebia deltaura*) (Miller et al., 1977; Taylor et al., 2000), as well as in *C. californiensis* (Blair and van Holde, 1976). In this case, the equilibria between different aggregation states (1×6-mer, 2×6-mer, 4×6-mer) appear to be governed by both divalent cations and temperature. In the SEC-FPLC chromatographic pattern of *U. pusilla* Hc, a small shoulder is visible as broadening of the main 4×6-meric Hc peak, suggesting the presence of a 2×6-

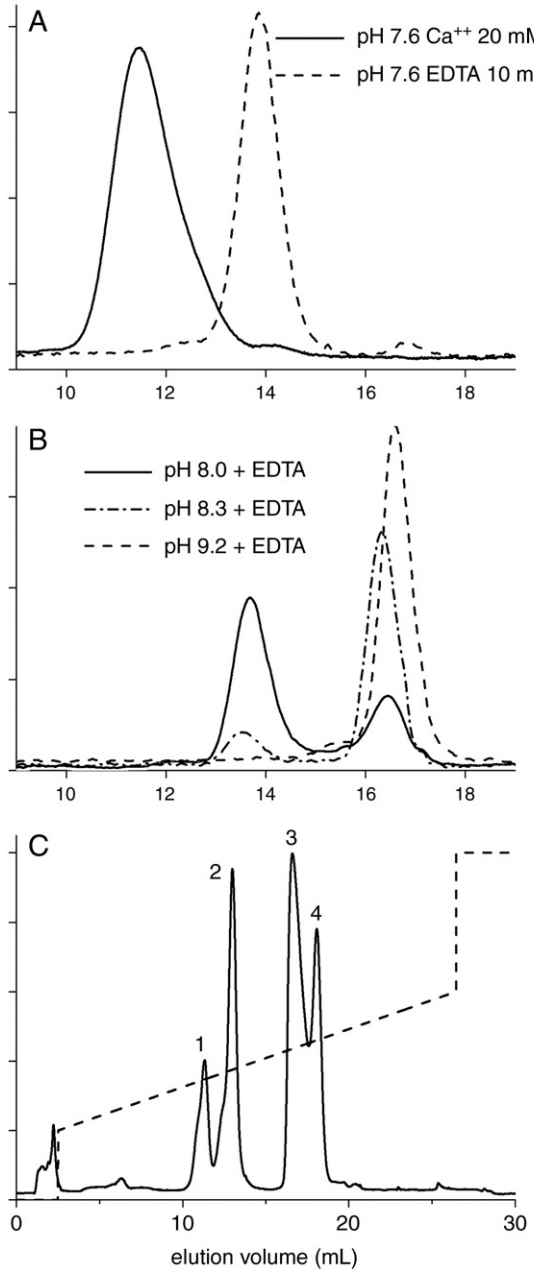

Fig. 4. Elution profiles of *Upogebia pusilla* hemocyanin under different pH and ionic conditions. The column (Superose 6 10/300) was previously calibrated with four known markers: a 4×6, a 2×6, a 1×6 hemocyanin and a subunit (data not shown). The *U. pusilla* hemocyanin sample was purified by preparative ultracentrifugation. A: elution profiles at pH 7.6 in the presence of Ca^{2+} 20 mM (solid line) or of EDTA 10 mM (dashed line); B: elution profiles in the presence of EDTA 10 mM and upon increasing the pH as indicated (elution profiles are not normalized to the same protein concentration, to avoid crowding of the figure); C: ion exchange chromatography of the monomeric fraction (obtained as in B at pH 9.2), Resource Q column equilibrated with 50 mM Tris/HCl buffer, EDTA 10 mM pH 9.2 and eluted with a continuous 20–60% NaCl gradient as indicated.

meric aggregation state. In the presence of EDTA this becomes visible as a distinct shoulder (Fig. 4A, B). This material, also evident from ultracentrifugation analysis, is present together with the 4×6-meric Hc in other thalassinidean shrimps. The issue is whether it represents an intermediate form in equilibrium with the 4×6-meric one, as expected for a dissociation intermediate (Taylor et al., 2000), or a different Hc pool needs further investigation. Dissociation of hexamers into monomers occurs upon increasing the pH in the presence of EDTA and full dissociation into monomers is observed at pH 9.2, which seems to be the case for all arthropod Hc (Fig. 4B).

The *U. pusilla* Hc was further analyzed by ion exchange chromatography, again under dissociating conditions (Fig. 4C). For this analysis, the peak of the monomeric protein obtained by SEC-FPLC as in Fig. 4B was run on an ion exchange column in the same buffer. The four peaks (1–4) of Fig. 4C show the typical oxy-Hc spectrum with A_{337}/A_{280} absorbance ratios of 0.21, 0.18, 0.22, 0.20, respectively. They can be interpreted as four different monomeric fractions. In agreement, SDS-PAGE reveals a 4-band pattern of monomers referred to as Up1 (78.9 kDa), Up2 (76.0 kDa), Up3 (69.8 kDa) and Up4 (67.1) (see inset Fig. 1). This marked heterogeneity in the monomeric fraction, is typically found both in Crustacea and Chelicerata Hcs (Markl, 1986). The dissociation process is reversible and reassociation of hexamers into 4×6-meric whole molecules occurs at pH 7.6 already at 1 mM $CaCl_2$ (data not shown).

3.2. Oxygen-binding properties

Upogebia pusilla Hc exhibits sigmoid oxygen-binding curves typical of a cooperative process. In the presence of 100 mM Tris/HCl, 20 mM $CaCl_2$ pH 7.6, that stabilizes the 4×6-meric aggregation form, $P_{50}=6.5\pm0.5$ kPa and $n_{max}=4.1\pm0.3$ are calculated. The oxygen-binding properties of crustacean Hcs are typically regulated by H^+ ions, lactate and urate that act as heterotropic allosteric effectors. In the case of the 4×6-meric Hc of chelicerates only the regulation by protons is observed and, for Hc from *E. californicum*, also by Tris (Paul et al., 1994; Sterner et al., 1994) and osmotic pressure (Hellmann et al., 2003). The oxygen-binding behaviour of *U. pusilla* Hc shows the typical effect of H^+ ions as expected for a crustacean Hc. Upon decrease of the pH to 7.2 in the same buffer-system, the affinity for oxygen decreases from $P_{50}=6.5\pm0.5$ kPa to $P_{50}=18.5\pm0.5$ kPa. The Bohr coefficient ($\triangle \mathrm{Log}P_{50}/\triangle \mathrm{pH}=-1.18$) falls in the same range as found for a number of other thalassinidean Hcs, $-1.06<(\triangle \mathrm{Log}P_{50}/\triangle \mathrm{pH})<-1.48$ (Taylor et al., 2000; Sanders and Childress, 1992; Miller et al., 1977), although its value is larger than that found for the other upogebid shrimp *U. pugettensis* (Miller et al., 1977). A marked effect on n_{max} is found by changing the proton concentration since this value falls to $n_{max}=2.7\pm0.1$ upon decreasing the pH from 7.6 to 7.2. With respect to this effect on n_{max}, *U. pusilla* represents a peculiar case since no effect of pH was found for a number of different species of thalassinidean shrimps (Taylor et al., 2000). Also the marked effect of lactate – decrease of cooperativity ($n_{max}=2.50\pm0.14$ at 20 mM lactate) and increase of affinity ($P_{50}=0.87\pm0.1$ kPa at 20 mM lactate) – makes *U. pusilla* Hc again a peculiar case compared to the other thalassinidean shrimps whose Hc does not exhibit a lactate effect (Taylor et al., 2000). No significant effect of urate on the oxygen-binding properties for this Hc could be detected in contrast to a number of other crustacean Hcs: urate has no significant effect on the cooperativity ($n_{max}=4.1\pm0.1$ in the absence of urate, $n_{max}=4.0\pm0.1$ in the presence of 0.40 mM

urate) and the effect on the affinity (P_{50}=6.5±0.5 kPa in the absence of urate, P_{50}= 5.0±0.5 kPa in the presence of 0.40 mM urate) is negligible.

3.3. Conclusions

In conclusion, the occurrence of the 4×6-meric aggregation state as distinct feature of thalassinidean shrimps further supports the view that within Crustacea different oligomeric forms of Hcs exist which are species-specific. Furthermore, the structure of the 24-meric forms of Hc differs within the *taxa* Crustacea and Chelicerata.

– The Hc of *U. pusilla* is formed by 1×6-meric building blocks without preferential interactions within pairs of hexamers. Thus, under our experimental conditions, only hexamers can be isolated along the dissociation pathway of the molecule. In contrast, Hc from Chelicerata shows a hierarchical assembly of 2×(2×6)-mers. It can be proposed that such aggregation forms were evolved independently within the two *taxa* from a basic hexameric structure. The two alternative ways of assembling these hexamers can be considered as the result of selective pressures that seem to operate at the level of interactions among constant building blocks rather than the generation of new structures.
– With respect to modulation of oxygen-binding properties by allosteric effectors no typical thalassinidean pattern can be found: protons in general have an effect on affinity, but not in all cases on n_{max}, and L-lactate has an effect only in some thalassinidean species. Thus, these evolutionary processes have produced aggregates that are differently modulated in their oxygen-binding properties by allosteric effectors as a consequence of a species-specific adaptation effects. A further analysis in the functional properties of *U. pusilla* Hc is still in progress.

Acknowledgments

The excellent technical assistance of Mr. Giuseppe Tognon (CNR) for electron microscopy is gratefully acknowledged. This work was also supported by Erasmus project for mobility (M.P.).

References

Arisaka, F., van Holde, K.E., 1979. Allosteric properties and the association equilibria of hemocyanin from *Callianassa californiensis*. J. Mol. Biol. 134, 41–73.

Bijholt, M.M., van Heel, M.G., van Bruggen, E.F., 1982. Comparison of 4×6-meric hemocyanins from three different arthropods using computer alignment and correspondence analysis. J. Mol. Biol. 161, 139–153.

Blair, D., van Holde, K.E., 1976. Sedimentation equilibrium studies of a complex association reaction. Biophys. Chemist. 5, 165–170.

Cavellec, A., Boisset, N., Taveau, J.-C., Lamy, J.N., 1990. Image processing of electron-microscopy views of *Callianassa californiensis* hemocyanin. In: Preaux, G., Lontie, R. (Eds.), Invertebrate Dioxygen Carriers. Leuven Univ. Press, Leuven, pp. 271–274.

Dainese, E., Di Muro, P., Beltramini, M., Salvato, B., Decker, H., 1998. Subunits compositions and allosteric control in *Carcinus aestuarii* hemocyanin. Eur. J. Biochem. 256, 350–358.

Ellerton, H.D., Ellerton, N.F., Robinson, H.A., 1983. Hemocyanin—a current perspective. Prog. Biophys. Mol. Biol. 41, 143–248.

Erker, W., et al., 2006. Immobilization and AFM of single 4×6-mer tarantula hemocyanin molecules. Micron 37, 735–741.

Hellmann, N., Raithel, K., Decker, H., 2003. A potential role for water in the modulation of oxygen-binding by tarantula hemocyanin. Comp. Biochem. Physiol., A Mol. Integr. Physiol. 136, 725–734.

Lamy, J., Bijholt, M.C., Sizaret, P.Y., Lamy, J., van Bruggen, E.F., 1981. Quaternary structure of scorpion (*Androctonus australis*) hemocyanin. Localization of subunits with immunological methods and electron microscopy. Biochemistry 20, 1849–1856.

Loewe, R., 1978. Hemocyanins in spiders. V. Fluorimetric recording of oxygen binding curves and its application to the analysis of allosteric interactions in *Eurypelma californicum* hemocyanin. J. Comp. Physiol. 128, 161–168.

Mangum, C.P., 1983. On the distribution of lactate sensitivity among hemocyanins. Mar. Biol. Lett. 4, 139–149.

Markl, J., 1986. Evolution and function of structurally diverse subunits in the respiratory protein hemocyanin from arthropods. Biol. Bull. 171, 90–115.

Markl, J., Schmid, R., Czichos-Tiedt, S., Linzen, B., 1976. Haemocyanins in spiders III Chemical and physical properties of the proteins in *Dugesiella* and *Cupiennius* blood. Hoppe Seyler's Z. Physiol. Chem. 357, 1713–1725.

Markl, J., Savel, A., Linzen, B., 1981. Hemocyanins in spiders XIV Subunit composition of dissociation intermediates and its bearing on quaternary structure of *Eurypelma* hemocyanin. Hoppe Seyler's Z. Physiol. Chem. 362, 1255–1262.

Markl, J., Decker, H., Linzen, B., Schutter, W.G., van Bruggen, E.F., 1982. Hemocyanins in spiders, XV The role of the individual subunits in the assembly of *Eurypelma* hemocyanin. Hoppe Seyler's Z. Physiol. Chem. 363, 73–87.

Markl, J., Decker, H., 1992. Molecular structure of the arthropod hemocyanins. Adv. Comp. Environ. Physiol. 13, 325–376.

Martin, A.G, et al., 2007. *Limulus polyphemus* hemocyanin: 10 Å cryo-EM structure, sequence analysis, molecular modelling and rigid-body fitting reveal the interfaces between the eight hexamers. J. Mol. Biol. 366, 1332–1350.

Miller, K., van Holde, K., 1974. Oxygen binding by *Callianassa californiensis* hemocyanin. Biochemistry 13, 1668–1674.

Miller, K., van Holde, K., 1982. Haemocyanins. Q. Rev. Biophys. 15, 1–129.

Miller, K.J., Eldred, N.W., Arisaka, F., van Holde, K.E., 1977. Structure and function of hemocyanin from thalassinid shrimp. J. Comp. Physiol. 115, 171–184.

Paul, R., et al., 1994. Gas transport in the haemolymph of arachnids — oxygen transport and the physiological role of haemocyanin. J. Exp. Biol. 188, 25–46.

Roxby, R., Miller, K., Blair, D.P., van Holde, K.E., 1974. Subunits and association equilibria of *Callianassa californiensis* hemocyanin. Biochemistry 13, 1662–1668.

Sanders, N.K., Childress, J.J., 1992. Special effects of thiosulphate and l-lactate on hemocyanin-O_2 affinity in a brachyuran hydrothermal vent crab. Mar. Biol. 113, 175–180.

Savel-Niemann, A., Markl, J., Linzen, B., 1988. Hemocyanins in spiders XXII Range of allosteric interaction in a four-hexamer hemocyanin Co-operativity and Bohr effect in dissociation intermediates. J. Mol. Biol. 204, 385–395.

Sterner, R., Bardehle, K., Paul, R., Decker, H., 1994. Tris: an allosteric effector of tarantula haemocyanin. FEBS Lett. 339, 37–39.

Taylor, A.C., Astall, C.M., Atkinson, R.J.A., 2000. A comparative study of the oxygen transporting properties of the haemocyanin of five species of thalassinidean mud-shrimps. J. Exp. Mar. Biol. Ecol. 244, 265–283.

Voit, R., Feldmaier-Fuchs, G., Schweikardt, T., Decker, H., Burmester, T., 2000. Complete sequence of the 24-mer hemocyanin of the tarantula *Eurypelma californicu* Structure and intramolecular evolution of the subunits. J. Biol. Chem. 275, 39339–39344.